Exchange and correlation effects on the ground states of quantum wires

D. Schmerek and W. Hansen
Institut für Angewandte Physik, Universität Hamburg, Jungiusstrasse 11, 20355 Hamburg, Germany
(Received 19 March 1999)

Recent results of capacitance measurements on one-dimensional quantum wires are numerically modeled. Local density approximation is used to take into account exchange and correlation effects. Particular attention is paid to the behavior at low densities close to the onset of the quantum wires, where measurements have revealed a pronounced enhancement of the capacitance signal. From the simulation results we infer that the enhancement is caused by exchange and correlation effects of the interacting one-dimensional electron gas. [S0163-1829(99)13031-5]

Exchange and correlation effects strongly depend on the dimension of the electron system.[1,2] In two-dimensional systems the most prominent consequence is the fractional quantum Hall state at high magnetic fields.[3] So far only few experimental systems with electron quantum wires have been realized with sufficient quality so that they are still well defined at very low electron densities at which strong many-particle effects on the ground state may be expected. In recent investigations of field-induced quantum wires in GaAs heterostructures a pronounced structure in the capacitance spectra close to the onset voltage has been observed.[4] It was tentatively associated to many-particle effects.[5] In this paper we present results of simulation calculations of the capacitance in quantum wires that strongly support this assertion.

We investigate field-effect-induced quantum wires in so-called metal insulator semiconductor (MIS) devices that are optimized for investigations of electron systems at low densities.[4,6] A typical sample design is sketched in Fig. 1. The device consists of a GaAs/AlAs heterostructure with a metal gate at the surface that is microstructured with high resolution *e*-beam lithography. Details of the fabrication are published elsewhere.[4] In these structures a high-mobility electron system is induced beneath the gate at the heterojunction at sufficiently large gate voltages. The gate electrode is biased with respect to a so-called back electrode that consists of a highly doped epitaxial GaAs layer buried beneath the heterojunction. This back electrode is the only doped layer in the system. It is separated from the electron system under investigation by a typically 100-nm thick undoped GaAs spacer layer. We thus expect that ionized donor potentials have only little effect on the low-dimensional electron system even at very low electron densities. In the case of Fig. 1 the gate consists of two pieces biased with voltage V_1 and V_2, respectively. As depicted the center gate forms a stripe beneath which a narrow electron channel is induced at sufficiently high voltages V_1. A tuning-fork-shaped side gate surrounding the center gate controls the confinement of the electron channel. This gate is biased at a voltage V_2 with respect to the gate electrode in order to squeeze the electron channel to very narrow quantum wires. In the data discussed here the voltage difference is kept constant at $V_1 - V_2 = 0.8\,\mathrm{V}$.

The successful concept of the above devices is, e.g., demonstrated with capacitance spectroscopy.[4,7] Dashed lines in Fig. 2 reflect typical results of capacitance measurements on single wire devices. The geometry of the gates in this particular device corresponds to the values denoted in Fig. 1. The barrier between the electron channels and the front gate is 42 nm thick, the distance between the front gate and back electrode is 142 nm. The differential capacitance is measured with a capacitance bridge by slightly modulating the voltage V_1 with an excitation $\delta V = 2$ mV at a frequency of 100 kHz. Different traces are taken at different magnetic fields ranging from zero to 5.0 T. The steep rise of the capacitance at $V_1 = 0.75\,\mathrm{V}$ reflects the onset of the quantum wire. At higher voltages further capacitance steps are clearly resolved reflecting the population of successive one-dimensional subbands. It may be instructive to note, that as expected from a single particle model the voltage range in which the system is in the one-dimensional quantum limit increases with the magnetic field. Similar to previous publications[4,7,8] this behavior can be analyzed yielding a sub-band spacing of 4.4 meV and a wire capacitance of 141 pF/m.

In all spectra a supplementary structure is clearly observed close to the onset of the quantum wire. In similar samples with a wider electron channel[9] or with two-dimensional electron systems[10,11] a corresponding structure at the onset is not observed. So far, the origin of this structure was not well understood. In particular, to resolve the nature of this structure, we modeled our system with a self-consistent Poisson-Schrödinger solver using the local density approximation (LDA).[12]

In our model calculations the wire is assumed to be ori-

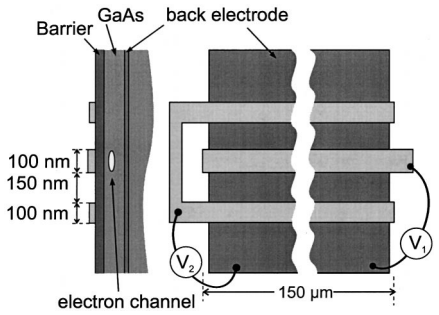

FIG. 1. Cross section and top view of a MIS heterojunction device for investigation of electron quantum wires. In the top view, light areas represent the front electrodes and the shaded area represents the back contact.

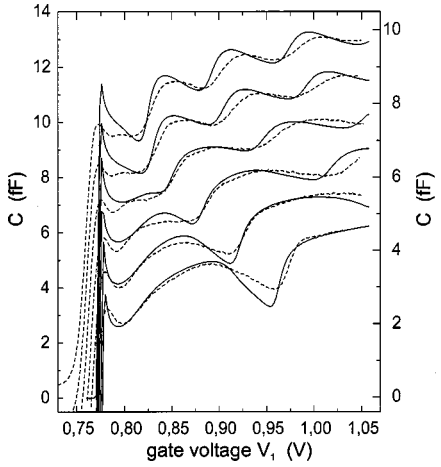

FIG. 2. Measured (dashed lines) and calculated (full lines) capacitance traces of a MIS device with parameters as specified in Fig. 1, and in the text. The scale on the left-hand side of the frame corresponds to the calculated traces, the scale on the right hand side is associated to the experimental data. A magnetic field is applied perpendicular to the sample surface. The topmost trace corresponds to $B=0$. The lower traces are offset by -2 fF for clarity and the field is increased in steps of 1 T each time. The voltage bias of the side gate V_2-V_1 is kept constant at $V_2-V_1=0.8$ V while V_1 is swept.

ented along the y axis and z is the direction of the magnetic field (perpendicular to the surface of the sample). Using $\psi_{jk_y}(x,y,z)=e^{ik_y y}\zeta_{jk_y}(x,z)$ for the single particle wave functions and $\vec{A}=B_z x\vec{e}_y$ for the vector potential leads to a Schrödinger-type equation,

$$\left\{-\frac{\hbar^2\triangle}{2m^*}+V_0(x,z,k_y)+V_H(x,z)+V_{xc}(x,z)\right\}\zeta_{jk_y}=E_{jk_y}\zeta_{jk_y},$$

which is solved simultaneously with the Poisson equation

$$\nabla[\epsilon\nabla V_H(x,z)]=-e\rho(x,z)$$

with

$$\rho=\frac{-e}{\pi}\sum_j\int_{-\infty}^{\infty}dk_y|\zeta_{jk_y}|^2\left[\exp\left(\frac{E_{jk_y}-\mu}{k_BT}\right)+1\right]^{-1}.$$

Here V_H is the Hartree potential and V_{xc} is the exchange-correlation part of the electron interaction potential. $V_0(x,z,k_y)=V_{ext}(x,z)+V_B(x,k_y)$ is the sum of the bare, i.e., unscreened, electrostatic confinement potential and the potential that is induced by the magnetic field. The latter is given by

$$V_B(x,k_y)=\frac{1}{2}m^*\omega_c^2\left(x-x_0-\frac{\hbar k_y}{m^*\omega_c}\right)^2$$

with $\omega_c=eB/m^*$. The capacitance is evaluated with Gauss' Law

$$C=-L\epsilon\frac{\partial}{\partial V_1}\left(\oint_\Gamma\vec{\nabla}(V_{ext}+V_H)\cdot\vec{n}ds\right),$$

where L is the length of the quantum wire, the path Γ encloses the center electrode, and $\vec{n}$ is the unit normal vector on Γ.

The full lines in Fig. 2 represent capacitance traces that we calculate with the parametrization of the exchange-correlation potential given in Hedin and Lundqvist:[13]

$$V_{xc}(x,z)=-\frac{1.22}{r_s}\mathrm{Ry}^*\left[1+3.68\cdot10^{-2}r_s\ln\left(1+\frac{21}{r_s}\right)\right],$$

where

$$r_s(x,z)=\left[\tfrac{4}{3}\pi a^{*3}\rho(x,z)\right]^{-1/3}$$

is the Wigner-Seitz radius. Furthermore, $a^*\approx10$ nm and $\mathrm{Ry}^*\approx5.6$ meV are the effective Bohr radius and Rydberg in GaAs, respectively. Though application of the local density scheme should be restricted to situations with a slowly varying density, it is well known that the method works surprisingly well even for systems beyond this limit.

For our calculations we use as input parameters the above-described gate geometry and heterostructure layer thicknesses that are known from the fabrication process within an error of about 10%. Diriclet boundary conditions are applied 800 nm above the surface of the device assuming vacuum in this region. With these parameters we find already fairly good qualitative agreement between measurement and simulation.

However, in order to reproduce the exact threshold voltage and onset voltages of the higher one-dimensional subbands, we have to make further assumptions about a homogeneous oxide layer on the surface of the sample as well as a distinct distribution of surface charges close to the gates. The thickness of the oxide layer influences the height of the calculated capacitance as well as the threshold voltage. Surface charges also influence the threshold voltage and they are shifting the onsets of the higher one-dimensional sub-bands. For example, the simulations yield a threshold voltage that is about 0.3 V higher and an absolute capacitance, which is about twice as high as the measured one if we do not assume any surface charges or an oxide layer. Furthermore, the separations between the sub-band onsets are smaller than the experimental ones by about 30% and more uniform. Although it is of minor importance for the interpretation of the capacitance structure at the wire onset we have chosen parameters for the oxide thickness and surface-charge distribution in order to achieve good quantitative agreement to the data with respect to the threshold voltage and separations of the sub-band onsets. For the calculated capacitance traces in Fig. 2 we assume the following charge distribution: The open semiconductor surface apart from the gate electrodes contains a surface-charge density of -1.8×10^{12} e/cm^2. A 15-nm wide stripe beside the electrodes contains a surface charge of 1.0×10^{13} e/cm^2. Assuming positive charges directly beside the gate electrodes is consistent with results of capacitance measurements on broader electron wires, which show a sub-threshold structure if the side gate voltage is small.[9] We think that the surface charges used in the simulation may reflect strain effects of the gate metal on the heterostructure.[14] Furthermore, a 2.5-nm thick oxide layer with dieletric constant of 3.0 is assumed to cover the semiconductor.

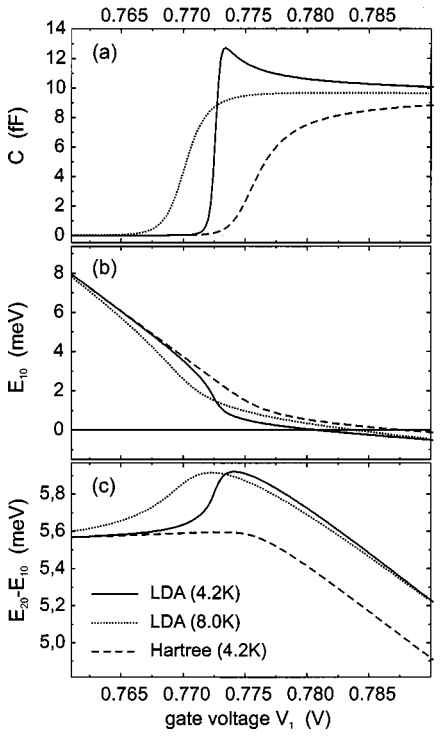

FIG. 3. Differential capacitance (a), energies of the lowest one-dimensional subband (b), and subband separation (c), calculated with a self-consistent Schrödinger-Poisson solver at gate voltages close to the threshold of the quantum wire. It is assumed that no magnetic field is applied; $V_2 - V_1$ is held constant at 0.8 V while V_1 is swept. The dashed line is calculated in Hartree approximation assuming a temperature $T = 4.2$ K. The full and dotted lines are calculated in LDA assuming temperatures $T = 4.2$ K and 8.0 K, respectively.

With the above assumptions we obtain good agreement with the experimental data concerning the position of the threshold voltage and the onset voltages of the higher subbands. We note that in Fig. 2 the scales of the simulated and experimental capacitances are different by about 30%. However, the absolute value of the capacitance measured with our bridge is not known with good accuracy, since it depends on parasitic capacitances at the balance point of the bridge that has been determined in theses measurements to an accuracy of about 25%. Thus, even the absolute values of the experimental and the calculated data correspond within the expected accuracy.

At the onset of the capacitance there is a very sharp peak in the calculated capacitance traces. We believe that it corresponds to the peak structure in the experimental data at low electron densities. As is obvious from traces in Fig. 2 the experimental capacitance at the onset is significantly broadened as compared to the calculated one. In the experiment, threshold variations along the wire cause such inhomogeneous broadening that is not included in the calculations. Since it also affects the line shape of the peak structure at the onset we do not expect perfect quantitative coincidence of the calculated and experimental traces in this region. In the following we demonstrate that the peak is originated by many particle effects.

In Fig. 3(a) calculated capacitances are depicted with an enlarged gate voltage scale. For comparison data calculated

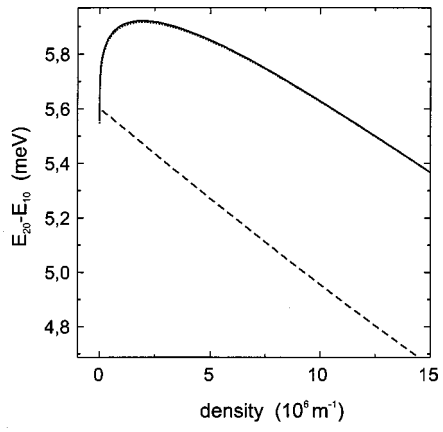

FIG. 4. Calculated subband separation as a function of electron occupation of the quantum wire. Dashed line denotes the result of a calculation in Hartree approximation. Full and dotted lines almost coincide and denote the LDA results for $T = 4.2$ K and $T = 8.0$ K, respectively.

for temperatures $T = 4.2$ K and 8.0 K are depicted together with a trace in which only Hartree approximation has been applied. The full and dashed lines are calculated in LDA and Hartree approximation, respectively. The dashed line does not reproduce the capacitance peak at the onset of the quantum wire. We thus associate the peak to exchange and correlation effects. The origin of the enhanced capacitance can be understood with the aid of Figs. 3(b) and 3(c). Figure 3(b) presents the energies of the lowest sub-band in the corresponding approximations. In Fig. 3(c) the energy separation between the edges of the two lowest one-dimensional subbands are depicted. The energies coincide as long as the wire remains unoccupied. Close to the threshold, however, the sub-band energy calculated in LDA is seriously reduced with respect to the energy calculated in the Hartree approximation. Exchange and correlation lead to a significant reduction of the ground-state energy at low electron density,[2] so that the capacitance onset is shifted to smaller gate voltages. Furthermore, the quantum wire is filled more rapidly in LDA. The capacitance is enhanced with respect to the value at higher electron densities where the Hartree contribution dominates the electron-electron interaction energy. The dashed line in Fig. 3(c) reflects the well-known result of Hartree calculations; that is the effective confinement potential widens due to screening once electrons are filled into the wire. Thus, the subband separation decreases monotonically. In contrast in LDA the subband spacing first rapidly increases at the onset before it decreases at higher electron densities. This reflects the fact that the lowest sub-band energy is most strongly affected by exchange-correlation effects.

In Fig. 4 the subband spacing is depicted as a function of the one-dimensional electron density in the quantum wire. In LDA the subband spacing goes through a maximum at a density of 1.8×10^6 m^{-1}. Below this density the exchange and correlation energy dominate the electron-electron interaction. We note that the two traces calculated in LDA for $T = 4.2$ K and 8.0 K can be hardly separated in Fig. 4. However, if the sub-band energies are drawn as a function of gate voltage as in Fig. 3 the energies are significantly different at different temperatures. In particular, the capacitance en-

hancement is not present any more. Instead the threshold is shifted to even lower gate voltages. It is obvious that thermal smearing of the quantum wire occupation reduces the many-particle interaction-induced capacitance enhancement.

In conclusion, we present results of self-consistent numerical calculations to model experimental capacitance traces of one-dimensional quantum wires. The calculations were motivated by a significantly enhanced capacitance observed at the quantum wire onset, which has been unexplained so far. Typical subband spacings of 5 meV are found. The oscillator length of the single-particle wave function in a parabolic potential with a subband spacing of 5 meV is of the same order as the Bohr radius in GaAs. We thus may expect correlation effects to become important at low density. Our calculations indeed demonstrate that the enhancement of the capacitance traces at the quantum wire onset is originated by exchange-correlation effects on the electronic ground state in the wires. The calculations suggest a strong temperature dependence, which presently is under experimental investigation. Within the accuracy to which input parameters of our model are known we achieve good agreement between measured and calculated data.

We note that in previous publications wider wires have been discussed where $l_0 \gg a^*$ and thus a classical approach can be used in high magnetic fields.[9,15] Furthermore, in our model the wire is assumed to be homogeneous along its axis (y direction). The average spacing between the electrons is similar to or larger than the oscillator length at densities where we find the pronounced capacitance enhancement. As has been pointed out previously, at such low densities, a Wigner-crystal-type correlation of electrons along the wire can also lead to a capacitance enhancement.[5] We expect this effect to become important at temperatures significantly lower than 4 K and in wires of very high quality.

We have profited from valuable discussions with C. Steinebach, A. O. Govorov, and A. Gold. We gratefully acknowledge financial support of the Deutsche Forschungsgemeinschaft via Project No. Ha2042/2 and the Sonderforschungsbereich 508 ''Quantenmaterialien.''

[1] J. Voit, Rep. Prog. Phys. **58**, 977 (1995).
[2] L. Calmels and A. Gold, Phys. Rev. B **56**, 1762 (1997).
[3] T. Chakraborty and P. Pietiläinen, in *The Fractional Quantum Hall Effect: A Survey of the Incompressible Quantum Fluid Including the Integer Quantum Hall Effect*, Springer Series in Solid-State Sciences, Vol. 85 (Springer, Berlin, 1995).
[4] H. Drexler, W. Hansen, S. Manus, J. P. Kotthaus, M. Holland, and S. P. Beaumont, Phys. Rev. B **49**, 14 074 (1994).
[5] A. O. Govorov, Solid-State Electron. **40**, 311 (1996).
[6] H. Drexler, W. Hansen, J. P. Kotthaus, M. Holland, and S. P. Beaumont, Semicond. Sci. Technol. **7**, 1008 (1992).
[7] W. Hansen and H. Drexler, *Festkörperprobleme Advances in Solid State Physics*, edited by R. Helbig (Vieweg, Braunschweig/Wiesbaden, 1996), Vol. 35, pp. 81–101.
[8] H. Drexler, W. Hansen, S. Manus, J. P. Kotthaus, M. Holland, and S. P. Beaumont, Phys. Scr. **T55**, 65 (1994).
[9] D. Schmerek, S. Manus, A. O. Govorov, W. Hansen, J. P. Kotthaus, and M. Holland, Phys. Rev. B **54**, 13 816 (1996).
[10] V. T. Dolgopolov, A. A. Shashkin, A. V. Aristov, D. Schmerek, H. Drexler, W. Hansen, J. P. Kotthaus, and M. Holland, Phys. Low-Dim. Struct. **6**, 1 (1996).
[11] V. T. Dolgopolov, A. A. Shashkin, A. V. Aristov, D. Schmerek, W. Hansen, J. P. Kotthaus, and M. Holland, Phys. Rev. Lett. **79**, 729 (1997).
[12] W. Kohn and L. J. Sham, Phys. Rev. **140**, A1133 (1965).
[13] L. Hedin and B. I. Lundqvist, J. Phys. C **4**, 2064 (1971).
[14] J. H. Davies and I. A. Larkin, Phys. Rev. B **49**, 4800 (1994).
[15] A. O. Govorov, Phys. Rev. B **51**, 14 498 (1995).